Contributions to Mineralogy and Petrology (2018) 173:65
https://doi.org/10.1007/s00410-018-1497-7

ORIGINAL PAPER

Formation by silicate–fluoride + phosphate melt immiscibility of REE-rich globular segregations within aplite dikes

Charles R. Stern[1] · Julien M. Allaz[1,3] · Markus B. Raschke[2] · G. Lang Farmer[1] · M. Alexandra Skewes[1] · Jeremy T. Ross[1,4]

Received: 29 March 2018 / Accepted: 16 July 2018 / Published online: 30 July 2018

Abstract

Aplite dikes intruding the Proterozoic 1.42(±3) Ga Longs Peak-St. Vrain Silver Plume-type peraluminous granite near Jamestown, Colorado, contain F, P, and rare earth element (REE)-rich globular segregations, with 40–46% REE, 3.7–4.8 wt% P_2O_5, and 5–8 wt% F. A combination of textural features and geochemical data suggest that the aplite and REE-rich globular segregations co-existed as two co-genetic liquids prior to their crystallization, and we propose that they are formed by silicate–fluoride + phosphate (+S + CO_2) melt immiscibility following ascent, cooling, and decompression of what was initially a single homogeneous magma that intruded the granite. The REE distribution coefficients between the silica-rich aplites and REE-rich segregations are in good agreement with experimentally determined distribution coefficients for immiscible silicate–fluoride + phosphate melts. Although monazite-(Ce) and uraninite U–Th–Pb microprobe ages for the segregations yield 1.420(±25) and 1.442(±8) Ga, respectively, thus suggesting a co-genetic relationship with their host granite, $\varepsilon_{Nd1.42Ga}$ values for the granites and related granitic pegmatites range from −3.3 to −4.7 (average −3.9), and differ from the values for both the aplites and REE-rich segregations, which range from −1.0 to −2.2 (average −1.6). Furthermore, the granites and pegmatites have $(La/Yb)_N$ <50 with significant negative Eu anomalies, which contrast with higher $(La/Yb)_N$ >100 and absence of an Eu anomaly in both the aplites and segregations. These data are consistent with the aplite dikes and the REE-rich segregations they contain being co-genetic, but derived from a source different from that of the granite. The higher $\varepsilon_{Nd1.42Ga}$ values for the aplites and REE-rich segregations suggest that the magma from which they separated had a more mafic and deeper, dryer and hotter source in the lower crust or upper mantle compared to the quartzo-feldspathic upper crustal source proposed for the Longs Peak-St. Vrain granite.

Keywords Silicate–fluoride + phosphate melt immiscibility · Rare earth elements · Aplites · Globular segregations · Jamestown, Colorado

Introduction

The rare earth elements (REE) are critical metals, which, because of their unique magnetic, electronic, optical and quantum properties, are used in a variety of technological applications such as REE-magnets, lasers and lighting, and catalysts (Chakhmouradian and Wall 2012). The formation of REE deposits related to igneous rocks is a complex function of their igneous source, magmatic crystallization and fractionation processes, hydrothermal modification and supergene enrichment during weathering (Chakhmouradian and Zaitsev 2012; Smith et al. 2016). Understanding the relative role of different magmatic processes is essential for understanding the formation of such deposits.

On the basis of a study of quartz-hosted micron-scale melt inclusions in the peralkaline Strange Lake granite,

Communicated by Timothy L. Grove.

Electronic supplementary material The online version of this article (https://doi.org/10.1007/s00410-018-1497-7) contains supplementary material, which is available to authorized users.

✉ Charles R. Stern
Charles.Stern@colorado.edu

[1] Department of Geological Sciences, University of Colorado, Boulder, CO 80309-0399, USA

[2] Departments of Physics, Chemistry, and JILA, University of Colorado, Boulder, CO 80309-0390, USA

[3] Present Address: ETH Zurich Institute für Geochemie und Petrologie, 8092 Zurich, Switzerland

[4] Present Address: United States Marine Corp, 3351 Onslow Drive, Camp Lejeune, NC 28547, USA

Northern Québec, Canada, Vasyukova and Williams-Jones (2014) proposed that silicate–fluoride melt immiscibility played an important role in concentrating the REE within this pluton. Vasyukova and Williams-Jones (2016) subsequently observed a macroscopic F-, REE-, and HFSE-rich ellipsoidal-shaped inclusion in this pluton which they suggested to have formed as a result of silicate–fluoride immiscibility. However, extensive post-crystallization hydrothermal alteration has recrystallized and redistributed elements in both the REE-rich ellipsoidal-shaped inclusion and host Strange Lake granite pluton (Gysi et al. 2016), obscuring many of the primary geochemical signatures of melt immiscibility, specifically the liquid–liquid partition coefficients of the REE between the inclusion and the granitic host.

To date, only two other occurrences of possible silicate–fluoride immiscibility in natural systems have been documented. For one, the Ary-Bulak ongonite intrusion, Eastern Transbaikal Region (Peretyazhko et al. 2007), no elemental partition coefficients have yet been determined. For the other, in mantle peridotite xenoliths from New Zealand (Klemme 2004, 2005), partition coefficients for REE between a fluoride and a silicate glass range from ~ 10 for La down to ~ 1 for all the other REE. However, the high pressure and temperature conditions for the formation within the mantle of these immiscible fractions are greatly different than those for upper crustal magmatic systems, and these distribution coefficients are significantly lower than those determined experimentally at low pressure (72–100 MPa) by Veksler et al. (2005, 2012), which trend progressively from ~ 200 for La down to ~ 100 for Yb.

Here we investigate the origin of macroscopic globular segregations (Fig. 1), with 40–46% REE, 3.7–4.8 wt% P_2O_5 and 5–8 wt% F (Table 1; Allaz et al. 2015), which occur in aplite dikes intruding the Longs Peak-St. Vrain Silver Plume-type granitic batholith near Jamestown, Colorado (Fig. 2; Goddard and Glass 1940; Allaz et al. 2015). To better understand the origin of these segregations, and their genetic relationship to their aplite host dikes and the Longs Peak-St. Vrain granite pluton, we have determined both the elemental and Nd-isotopic compositions of these different units. Our Nd-isotopic and trace-element data indicate that the aplite and the F-, P_2O_5-, and REE-rich segregations were co-genetic. We interpret textural features preserving various stages of agglomeration, coalescence and deformation of the segregations in the aplites (Fig. 1) as evidence that they co-existed as liquids prior to their crystallization. We suggest that they are formed by liquid immiscibility from a single initially homogeneous melt with a different source from the magmas that formed the Longs Peak-St. Vrain granite. This melt intruded the granite, and subsequently, upon cooling and decompression, separated into two immiscible liquids: (1) a silicate-rich melt which formed the aplite; and (2) a REE-rich fluoride + phosphate (± sulfide ± carbonate) melt with lower silica content forming the segregations.

Unlike the REE-rich Strange Lake peralkaline granite, neither the Longs Peak-St. Vrain granite, aplite dikes, nor the F-, P_2O_5- and REE-rich segregations has undergone subsequent hydrothermal alteration. Samples from this locality, therefore, provide a unique opportunity to evaluate the distribution of elements between immiscible silica–fluoride + phosphate melt fractions formed in a natural system, and to compare these with distribution coefficients for silicate–fluoride and silicate–phosphate melt immiscibility determined experimentally by Veksler et al. (2005, 2012). The results thus help constrain the conditions for concentrating REE and other incompatible elements by silicate–fluoride + phosphate melt immiscibility in magmatic systems, and the possible role of immiscibility in creating economically viable REE deposits.

Geologic setting

Goddard and Glass (1940) were the first to describe the unusual REE mineralization at a locality known as the "Rusty Gold" deposit within the Proterozoic 1.42(± 3) Ga Longs Peak-St. Vrain Silver Plume-type peraluminous granitic intrusion (Fig. 2; Peterman et al. 1968; Peterman and Hedge 1968; Anderson and Thomas 1985). The Longs Peak-St. Vrain pluton was emplaced at shallow depth (6–9 km; Anderson and Thomas 1985). The presence of Paleoproterozoic metasedimentary xenoliths (mainly ~ 1.8 Ga biotite schist; DePaolo 1981) further indicates that the studied outcrops are close to the margin of the intrusion (Goddard and Glass 1940). The Longs Peak-St. Vrain pluton and other Silver Plume-type intrusions are A-type peraluminous [Al/(Ca + Na + K) > 1.0], two-mica granites exhibiting enrichment in K and other incompatible elements (Rb, Ba, Th and LREE), and depletion in Ca and Mg compared to orogenic granites (Baker et al. 1976). The overall geochemistry suggests that the source of these intrusions was the melting of garnet-bearing high-grade quartzo-feldspathic continental crust (DePaolo 1981; Anderson and Thomas 1985).

The REE mineralization occurs at two spatially separate localities, approximately one kilometer apart, indicated by (1) and (2) on the map (Fig. 2). Goddard and Glass (1940) described the occurrence in these segregations of cerite, bastnäsite, monazite and allanite, as well as fluorite, quartz, uraninite, magnetite and sulfide phases. A misidentification of the cerite was first suggested based on an XRD analysis (Rabbitt 1952), and this mineral was later confirmed to be fluorbritholite-(Ce) by in situ microanalysis (Affholter 1987; Affholter and Adams 1987; Allaz et al. 2015). Allaz et al. (2015) provided a more detail description of the mineralogical complexity of samples from the northern locality, along

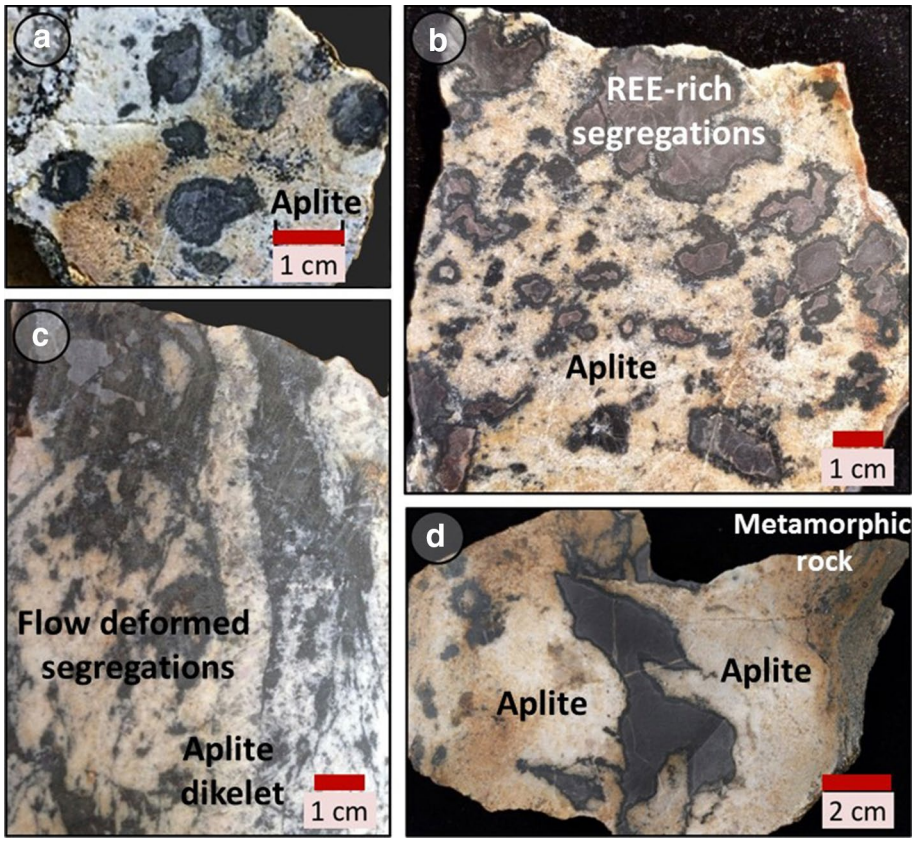

Fig. 1 Photographs of four texturally distinct REE-mineralized segregations within aplite. The segregations all consist of dark allanite-(Ce) rims surrounding somewhat lighter gray colored fluorbritholite-(Ce) + fluorite + monazite-(Ce) cores (Allaz et al. 2015). The aplite consists of dominantly plagioclase ($Ab_{70–85}$) along with lesser amounts of quartz, alkali feldspar and biotite (see Fig. 4). **a** Sample with individual isolated globular REE-mineralized pods, the largest of which is 11 mm in diameter with 1-mm-thick allanite rims. This was the type of sample ground-up and analyzed to determine the bulk rock composition of the hypersolvus magma prior to separation by silicate–fluoride + phosphate melt immiscibility of the F-, P- and REE-rich segregations from the silica-rich aplite. **b** A sample in which some of the small globular REE-rich segregations have agglomerated and coalesced into larger concentration of REE-rich material. **c** A sample with an even greater amount of agglomeration and coalescence of the globular REE-rich segregations, elongated and deformed possibly by flow in the aplite + segregation-bearing magma during intrusion into the host granite pluton. A thin aplite dikelet cuts the flow-deformed segregations. **d** Sample with one relatively large and several smaller lenses forming by agglomeration and coalescence of globules, and several small isolate globules of REE-rich material in aplite. The intrusive contact of the aplite with older metamorphic rocks occurs on the right side of the sample

with U–Th–Pb_{total} microprobe ages of monazite-(Ce) and uraninite at 1.420(± 25) and 1.442(± 8) Ga, respectively, which are, within error, identical with the Longs Peak-St. Vrain granite intrusion age. Neither Goddard and Glass (1940) nor Allaz et al. (2015) provided detailed petrochemical descriptions of the aplite dikes within which the REE-rich segregations occur, but both considered the aplites as well as the REE-rich segregation to be late-stage residual melts derived from and co-genetic with the Longs Peak-St. Vrain granite.

The aplite samples and REE-rich segregations described here are from the northern locality. Three separate exposures of different aplite dikes containing REE-rich segregations occur at this locality. These exposures are each of limited extent. Within one, which has been enhanced by a prospect trench, the aplite dike varies in thickness from 30 to 60 cm over a length of 2.5 m. In this outcrop, the aplite dike intrudes along the contact between the granite and a metasedimentary roof pendent (Fig. 1d).

The REE-rich segregations at this locality vary from relatively small (≤ 11 mm in diameter) isolated globules (Fig. 1a), to multiple aggregates of agglomerated and coalesced globules (Fig. 1b, c), to ≥ 5 cm thick vein-like lenses with up to ≥ 20 cm extension and with only minor internal relicts of globular textures (Fig. 1d). Both the REE-rich globular and vein-like segregations are formed by two visually distinct mineral zones (Fig. 1): a dark black rim (Zones #1 and #2; Allaz et al. 2015) primarily composed of dark green to brown allanite-(Ce) with minor monazite-(Ce), and a lighter gray to purple core

Table 1 Average compositions of rocks and the estimated composition of the segregations

Rock type	Granite	Pegmatite	Aplite	Core REE	Rims	0.55 core + 0.45 rim	Bulk rock
# samples	3	3	5	3	4		5
SiO_2	72.69	73.03	69.23	18.62	34.03	25.55	63.27
TiO_2	0.34	0.28	0.03	0.00	0.20	0.09	0.07
Al_2O_3	13.97	14.70	18.32	0.32	12.90	5.98	16.31
Fe_2O_3	2.14	1.82	0.65	0.32	13.40	6.21	2.67
MnO	0.02	0.04	0.02	0.30	0.81	0.53	0.16
MgO	0.49	0.33	0.13	0.02	0.63	0.31	0.53
CaO	0.47	0.49	2.86	14.32	8.44	11.67	4.42
Na_2O	2.34	0.93	5.56	0.02	0.18	0.09	3.75
K_2O	5.38	5.34	1.51	0.03	0.10	0.06	0.68
P_2O_5	0.16	0.38	0.15	4.66	1.68	3.31	0.46
F			0.16	6.85	0.32	3.91	0.47
LOI	1.52	2.19	1.03	3.91	1.56	2.71	1.91
Total	99.49	99.50	99.51	49.36	74.25	60.56	94.37
Cs	3.9	5.7	2	< 0.5	0.9	0.69	1.3
Rb	277	454	44	< 2	9	5.2	86
Ba	632	135	870	90	171	127	1185
Sr	148	24	1900	2133	593	1440	1866
Nb	18	71	3	< 1	7	3.6	8.9
Zr	247	141	35	31	17	25	40
Hf	5.5	3.7	1.0	9.7	3.8	7.1	1.5
Th	62.8	20.2	12.8	3230	1508	1456	359
Pb	34.0	20.7	92.6	1960	833	1453	
U	4.3	5.2	33.3	4113	845	2300	238
La	95.3	26.7	434	77,033	41,345	60,973	8165
Ce	217	63.7	799	221,333	104,880	168,929	20,694
Pr	26.8	8.12	126	26,100	12,355	19,915	2665
Nd	101	30.6	445	97,300	41,535	72,206	9112
Sm	16.8	6.70	54.4	12,200	4770	8857	1068
Eu	1.23	0.38	14.4	2460	867	1743	224
Gd	7.80	4.27	27.6	5313	1786	3726	563
Tb	0.87	0.80	2.85	537	184	378	52.3
Dy	4.10	5.00	12.0	2257	735	1572	200
Y	20	35	41	9472	3028	6573	802
Ho	0.70	1.03	1.65	333	100	226	22.9
Er	1.87	3.07	3.85	751	217	485	48.4
Tm	0.26	0.53	0.44	86.0	25.0	58.6	6.11
Yb	1.47	3.53	2.33	463	135	316	34.3
Lu	0.19	0.47	0.29	57.8	18.0	39.9	3.81
(La/Yb)N	44	5.1	127	113	209	131	162

(Zone #4; Allaz et al. 2015) composed primarily of fluorbritholite-(Ce) (> 50% modal), fluorite (10–25%), monazite (10–15%), and quartz (5%), with minor Fe-oxides and -sulfides, bastnäsite-(Ce) and REE-rich uraninite. The rim is further subdivided between a pure allanite outer domain (Zone #1; Allaz et al. 2015) and a monazite + allanite inner domain (Zone #2). A thin and irregular intermediate zone (Zone #3; Allaz et al. 2015) between the rim and the core can be present and is characterized by the presence of törnebohmite-(Ce), cerite-(Ce), and REE-carbonates consisting of mixtures of bastnäsite-(Ce) ± synchysite-(Ce), but devoid of fluorite. Minerals in the core of the segregations are mostly isogranular with a constant 120° dihedral angle at triple junction between all major phases. The cores of the segregations also contain small rounded clusters of monazite and fluorite in some instances surrounded

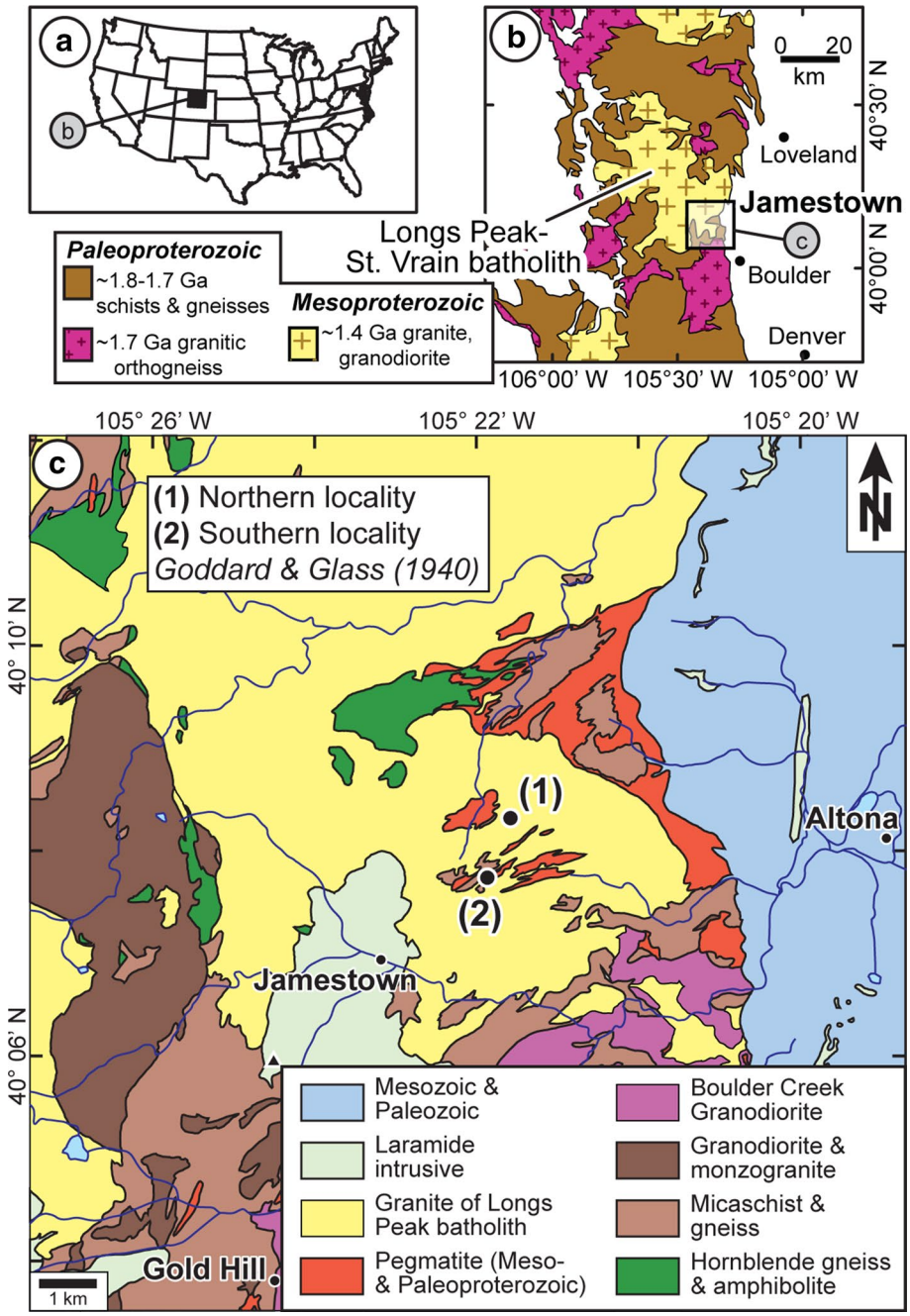

Fig. 2 Location maps modified from Allaz et al. (2015). **a** Map of the USA showing the location of map **b. b** General geological setting of the Mesoproterozoic intrusions within the front range of Colorado (simplified after Tweto 1979). **c** Modified geological map from Cole et al. (2009), with locations of the northern (1) and southern (2) localities of the REE mineralization originally described by Goddard and Glass (1940). The samples pictured in Fig. 1 and analyzed for this paper come from the northern locality

by pyrite and minor amounts of REE-rich carbonates (see Fig. 5 in Allaz et al. 2015).

Methods

Several samples each of Longs Peak-St. Vrain granite and pegmatites, aplites and the F-, P- and REE-rich segregations were analyzed for whole-rock major and trace-element contents by ICP-MS techniques at Activation Laboratories, Canada, and for Nd-isotopic ratios by solid-source mass-spectrometry at the University of Colorado as described by Farmer et al. (1991). Total bulk rock (aplite + REE-rich segregations) compositions have been determined for five samples in which the REE-rich globules remain small (≤ 11 mm) and isolated (Fig. 1a) and are not agglomerated (Fig. 1b, c) and/or coalesced into larger lenses (Fig. 1d). This was done by powdering large slabs (> 100 g) of these samples to capture representative proportions of the aplite and REE-rich globules.

Biotite and plagioclase chemistry was determined by electron microprobe analysis on a JEOL JXA-8600 electron

microprobe at the University of Colorado-Boulder. It is a four-spectrometer instrument equipped with argon X-ray detectors (P-10 mixture) on spectrometer 1 and 2 (PET and TAP crystals), and xenon X-ray detectors on spectrometers 3 and 4 (LiF crystals). Operating conditions using a W-cathode were 15 KV accelerating potential with a 20 nA probe current. A 5–10 µm beam was used to obtain the analysis on the biotites. F was analyzed at the beginning of the analysis sequence to minimize devolitization.

Results

Petrochemistry

Table 1 presents the average major and trace-element compositions for samples of Longs Peak-St. Vrain granite and granitic pegmatite samples collected in close vicinity to the northern REE-mineralized locality, for aplites, for the cores and rims of the REE-rich segregations, for the total bulk segregations as estimated in the proportions 55 wt % cores and 45 wt % rims, and for the composition of bulk samples of aplite and isolated globular REE-rich segregations. Compositions of individual samples of the different rock types are recorded in tables stored within the Electronic Supplementary Materials (ESM).

The two-mica Longs Peak-St. Vrain granite from the vicinity of the REE-mineralized localities has coarse porphyritic texture, with relatively large euhedral crystals of orthoclase perthite in a holocrystalline groundmass of hypidiomorphic quartz, Na-rich plagioclase ($Ab_{90–98}$), biotite, muscovite, and minor apatite, zircon and opaques. Granitic pegmatites have similar mineralogy as the granite, but with greater proportions of quartz, alkali feldspar and muscovite, along with occasional garnet and tourmaline. Biotites in the granite and pegmatites have 19.5–27.0 wt% FeO and 8.0–3.0 wt% MgO, with atomic Fe ≫ Mg, and 0.7–2.1 wt% F (ESM Table 1). The granites and pegmatites have low CaO and MgO contents (Table 1 and EDM Table 2) and Al/(Ca + Na + K) > 1.0 consistent with their classification as peraluminous granites similar to other Proterozoic Silver Plume-type intrusions (Anderson and Thomas 1985). Granites are LREE-enriched with average $(La/Yb)_N = 44$ and a significant negative Eu anomaly (Fig. 3). The pegmatites have lower LREE and average $(La/Yb)_N = 5.1$, but similar large negative Eu anomalies.

Aplites, in contrast to the granites, exhibit a distinctive fine-grained equigranular texture (Fig. 4), dominated by more Ca-rich plagioclase ($Ab_{70–85}$), along with minor quartz, alkali feldspar and small amounts of more Mg-rich biotite, as well as occasional monazite and allanite. No systematic spatial variations in mineralogy, modal mineral abundance or grain size have been observed in the aplites,

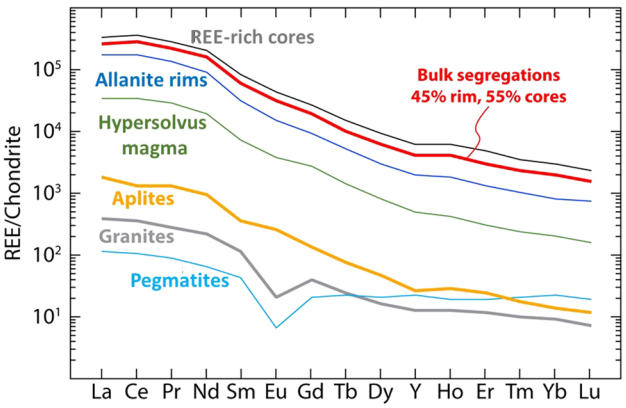

Fig. 3 Chondrite normalized REE contents (Table 1) of average granites, pegmatites, aplites, the cores, rims and total (45 wt% rims + 55 wt% cores) of the REE-rich segregations, and the hypersolvus magma as represented by bulk rock analysis of aplites containing isolated globular segregations such as the sample pictured in Fig. 1a

but modal proportions of biotite vary from 0 to 5 vol% and plagioclase varies from less than to greater than 50 vol% in different samples. The biotites in aplite have 11.8–18.8 wt% FeO and 16.5–10.2 wt% MgO, with atomic Fe < Mg, and 2.2–2.5 wt% F (ESM Table 1). Aplites have lower SiO_2 and K_2O and higher Na_2O, Al_2O_3 and CaO than the granites (Table 1 and ESM Table 3), which is reflected in their mineralogy and mineral chemistry by a greater abundance of more An-rich plagioclase relative to quartz and alkali feldspar. Further, the aplites have higher LREE content than the granites, but slightly lower HREE, and therefore, higher average $(La/Yb)_N = 127$, and no significant negative Eu anomaly (Fig. 3).

The cores of the REE-rich segregations have much lower SiO_2, Al_2O_3, Na_2O and K_2O than the aplites, and higher CaO, P_2O_5, F, and REE (Table 1 and ESM Table 4). However, they have similar average $(La/Yb)_N = 113$ compared to the aplites and also lack a negative Eu anomaly (Fig. 3). The allanite ± monazite rims of the REE segregations (Zones #1 and #2) have SiO_2, Al_2O_3, CaO, P_2O_5 and total REE intermediate between the aplite and core compositions, but have a distinctly higher Fe content and higher average $(La/Yb)_N = 209$ (Fig. 3; Table 1 and ESM Table 4). This is consistent with the rims not being a reaction zone between the cores and aplite, but instead having crystallized from the same REE-rich melt as which also formed the cores, as concluded previously by Allaz et el. (2015).

Table 1 also presents a calculated composition of a total REE-rich segregation prior to the separation of the allanite rims from the core, assuming weight proportions of 45% rim and 55% core. These weight proportions are based on (1) measurements of average rim thicknesses of typically 1 mm relative to a total segregation diameter of typically 11 mm (Fig. 1a), which then corresponds to the rims forming ~ 45%

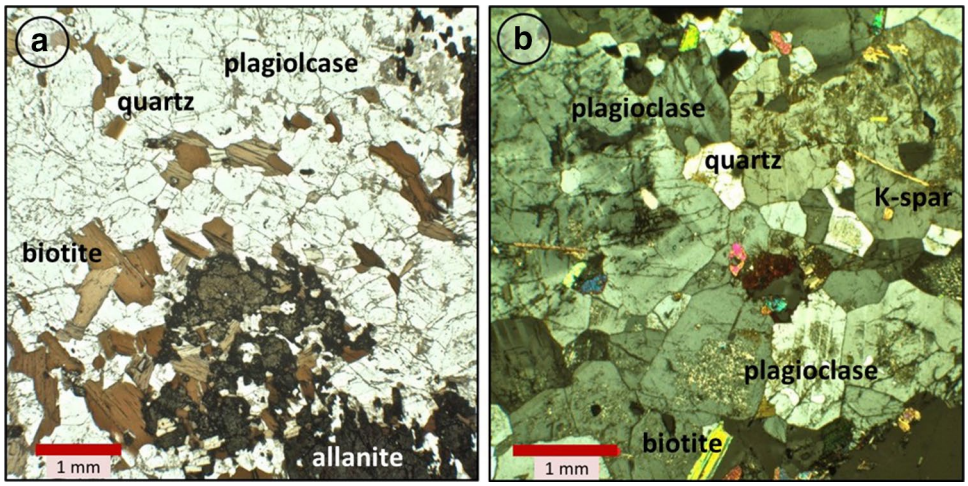

Fig. 4 Photomicrograph of **a** aplite sample JR-13 in plane polarized light, with a small amount of dark allanite-(Ce) in the lower right side of the sample; and **b** sample SK11 under crossed nicoles at higher magnification showing the distinctive granular texture in the dominantly plagioclase-rich ($Ab_{70–85}$) aplites

of the total volume of the segregations; and (2) our calculation, based on average mineral proportions and densities for both the rim and the core domains of the REE segregations, of similar approximate rim and core densities of between 4.0 and 4.2 g/cm^3, consistent with the higher REE-content of the core being balanced by the presence of low-density minerals such as fluorite and quartz. The composition of a total REE-rich segregation so calculated is similar to the analysis of one total segregation (sample REE4 in ESM Table 4).

The average composition (Table 1) of five bulk rock samples representative of the total composition of aplite + REE segregations (ESM Table 5) is andesitic, with ~ 5.5% total REE, $(La/Yb)_N = 162$ and no significant negative Eu anomaly (Fig. 3).

Nd-isotopic ratios

Nd-isotopic ratios were measured for two Proterozoic Idaho Springs Formation metamorphic country rocks, two granites, one pegmatite and two minerals (garnet and plagioclase) separated from a pegmatite located close to the REE-rich mineralization, and for two aplite and six mineralized samples (Table 2). For the latter, three samples are allanite-rich samples from the rims of the segregations, and three are samples from the core of the segregation. Two of these samples S1(Y) and SL1-3 are from the southern locality (2 in Fig. 2). S1(Y) is allanite, similar in chemistry to the rims of segregation from the northern locality, and SL1-3 is composed essentially of fluorbritholite-(Ce) (> 50% modal), fluorite (10–25%), monazite (10–15%), and quartz (5%) similar to the cores of segregations from the northern locality. The other four, as well as both aplite samples, are from the northern locality. Initial $\varepsilon_{Nd1.42Ga}$ values for the granites, pegmatites, aplites and REE-rich segregations were all calculated at 1422 Ma, and $\varepsilon_{Nd1.42Ga}$ for the metamorphic country rocks were also calculated at 1422 Ma to compare with the granites, aplites and REE-rich segregation at the time of their formation.

Initial $\varepsilon_{Nd1.42Ga}$ values for the granites and pegmatites range from − 3.3 to − 4.7 (Fig. 5) and average − 3.9 for five samples, below the low end of the range 0.0–− 3.0 determined for three samples of Silver Plume-type granites from Colorado by DePaolo (1981). In contrast, the aplite, and REE-rich segregations from both the northern and southern localities, have $\varepsilon_{Nd1.42Ga}$ which range from − 1.0 to − 2.2 (average − 1.6; Fig. 5), similar to each other but different from and higher than those of the granites and pegmatites. Initial $\varepsilon_{Nd1.8Ga}$ for the metamorphic country rocks calculated at 1800 Ma range from 1.5 to 1.6, which is slightly below the range 2.5–4.5 determined for other Proterozoic metamorphic rocks from Colorado by DePaolo (1981). Calculated at 1422 Ma the $\varepsilon_{Nd1.42Ga}$ values for the metamorphic rocks range from − 2.4 to − 3.5 (average − 3.0; Table 2), close to the range of the granites and consistent with similar metamorphic rocks possibly being the source from which the granites formed by partial melting (DePaolo 1981; Anderson and Thomas 1985; Smith et al. 1999).

Discussion

The geochemical data indicate that the aplite dikes and REE-rich segregations on the one hand, and the Longs Peak-St. Vrain granite and pegmatites on the other, had different sources with distinct isotopic and geochemical signatures. First, the average initial $\varepsilon_{Nd1.42Ga}$ values of the granites and associated pegmatites (− 3.9) differ significantly from that of the aplites and REE-rich segregations (− 1.6; Fig. 5). These isotopic differences imply that crystal-liquid fractionation could not have produced the aplites and REE-rich segregations from the granites as suggested previously by Goddard and Glass (1940) and Allaz et al. (2015). Second, the aplite and the granite display very different $(La/Yb)_N$ ratios

Table 2 Nd-isotopic data

Sample	Sm (ppm)*	Nd (ppm)[a]	$^{147}Sm/^{144}Nd$	$^{143}Nd/^{144}Nd$[b] (m)	ε_{Nd} (0)[c]	ε_{Nd} (T)[c]
Longs peak granite						
JR-3	11.3	70.1	0.0978	0.511540 ± 15	− 21.4	− 3.4
JR-11	4.40	19.5	0.1362	0.511859 ± 7	− 15.2	− 4.2
Country rock schist (1.8 GPa Idaho Springs Fm.)						
JR-9	5.99	31.5	0.1150	0.511754 ± 10	− 17.2	− 2.4
JR-10	21.7	140	0.0942	0.511503 ± 13	− 22.1	− 3.5
Pegmatite						
JR-8	8.87	28.2	0.1901	0.512406 ± 9	− 4.5	− 3.3
JR-18 feldspar	55.8	287	0.1177	0.511662 ± 18	− 19.0	− 4.7
JR-18 garnet	31.6	160	0.1194	0.511707 ± 11	− 18.2	− 4.1
Aplite						
SK-11	36.9	273	0.0818	0.511473 ± 9	− 22.7	− 1.8
JR-12	55.0	464	0.0717	0.511380 ± 8	− 24.5	− 1.8
REE-rich segregations						
C1 core	11,280	90,100	0.0757	0.511455 ± 7	− 23.1	− 1.0
A1 core	11,013	84,671	0.0787	0.511464 ± 6	− 22.9	− 1.4
SK15 rim	2715	34,070	0.0482	0.511136 ± 10	− 29.3	− 2.2
A1 rim	6585	55,224	0.0721	0.511398 ± 11	− 24.2	− 1.5
S1 (Y) rim	1811	16,461	0.0666	0.511348 ± 10	− 25.2	− 1.4
SL1-3 core	26,811	154,955	0.1047	0.511714 ± 10	− 18.0	− 1.3

Total procedural blanks averaged ~ 100 pg for Nd during study period

Analyses were dynamic mode, three-collector measurements. Thirty-two measurements of the La Jolla Nd Standard during the study period yielded a mean $^{143}Nd/^{144}Nd = 0.511840 \pm 1$ (2-σ μean)

ε_{Nd} (0) are measured (present-day) values, initial ε_{Nd} calculated at $T = 1422$ Ma

[a]Isotope dilution concentration determinations accurate to 0.5% for Sm and Nd

[b]Measured $^{143}Nd/^{144}Nd$ normalized to $^{146}Nd/^{144}Nd = 0.7219$

[c]ε_{Nd} values calculated using a present-day $^{143}Nd/^{144}Nd$ (CHUR) = 0.512638

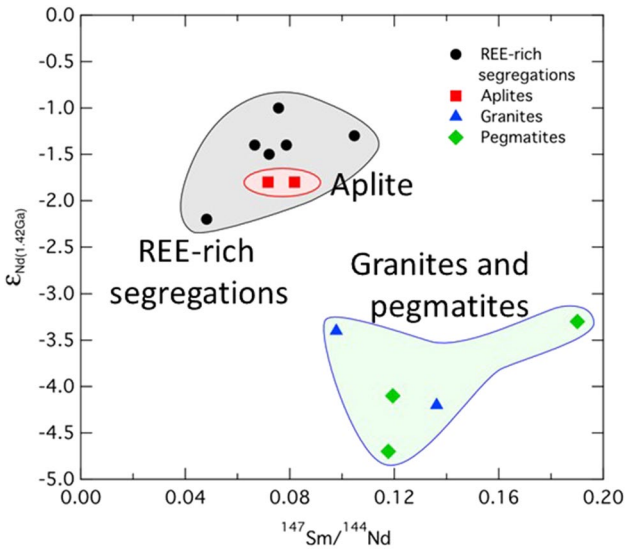

Fig. 5 Initial Nd-isotopic compositions (Table 2) versus $^{147}Sm/^{144}Nd$ of granites (triangles) and associated pegmatites (diamonds) compared to aplites (squares) and REE-mineralized segregations (circles)

and only the granitic materials show a negative Eu anomaly (Fig. 3). In contrast, the aplite and the REE-rich segregation have the same $\varepsilon_{Nd1.42Ga}$ and $(La/Yb)_N$ ratios despite very different REE contents, and both lack negative Eu anomalies, consistent with them being co-genetic.

We interpret the textural evidence for agglomeration, coalescence and deformation of the REE-rich globules in some sections of the aplite dikes (Fig. 1) to suggest that these globules and the aplites were both liquid at the time of intrusion, and that flow during the intrusion of these dikes acted to agglomerate, coalesce and deform the globule segregations within the aplite magma. Based, therefore, in part on their globular texture, as well as the textural and geochemical evidence that they co-existed as two co-genetic liquids prior to their crystallization, we suggest that the REE-rich segregations formed within an initially homogeneous magma due to the separation by liquid–liquid immiscibility of a fluoride + phosphate-rich melt from a silicate-rich aplitic melt fraction, the former partitioning most of the REE. Formation of the globular

REE-rich segregations by crystal-liquid fractionation of the aplite is inconsistent with the high modal proportion of plagioclase in the aplite and the lack of a negative Eu anomaly in the REE-rich segregations (Fig. 3). Also, the presence of K-feldspar along with minor monazite and allanite in the aplites (Fig. 4) would reduce the potential for crystal-liquid fractionation concentrating the REE greater than 100-fold into a residual melt as is required to produce the compositions of the observed REE-rich segregations.

We propose that immiscible separation took place as the hypersolvus magma, which had an andesitic composition (Table 1) and an independent origin from the granite, rose from its source and intruded, cooled, and decompressed near the roof of the Longs Peak-St. Vrain granite pluton. The presence in some section of the aplite dikes of isolated spherical globules of different sizes (Fig. 1a) suggests that these formed and solidified in situ, not at depth during uprise prior to intrusion, as they would then likely be deformed during the intrusion processes. Crystallization of the aplite and REE-rich segregations following immiscible separation must, therefore, have been relatively rapid for these samples that preserve isolated undeformed globulars (Fig. 1a). In contrast, the occurrence of larger pods and lenses formed by agglomerated, coalesced and flow-deformed globules (Fig. 1b–d) indicate that in other instances the aplite and globular REE-rich segregations remained in a liquid state longer during the intrusion and immiscible separation process. Ultimately, the F-, P_2O_5- and REE-rich liquids, that segregated from and in some cases coalesced within the aplite, crystallized progressively inward from the relatively Fe-rich allanite-(Ce) rims as described by Allaz et al. (2015).

The lack of post-crystallization hydrothermal alteration allows for the determination of the distribution coefficients (D = concentrations in the segregations/concentrations in the aplites) for both REE (Fig. 6) and other elements (Table 3), between what we propose to be the naturally occurring immiscible fractions, and for the comparison of these D values with those determined experimentally by Veksler et al. (2005, 2012) for both fluoride–silicate and phosphate–silicate systems. The D values determined for the REE and Y from both the natural and experimental systems are generally similar and all greater than two orders of magnitude (Fig. 6). For Fe_2O_3, Cs, Rb, Nb, Zr, Hf and U, the D values in the natural system fall in the range between the experimentally determined values in the fluoride–silicate and phosphate–silicate systems, in general being somewhat more similar to those in the fluoride–silicate system as are the D values for the REE and Y. However, D values for TiO_2, Al_2O_3, CaO, MgO, Na_2O, K_2O, Ba and Sr are all lower, and for Th higher in the natural system than either of the experimental systems. In the natural system there is also significant

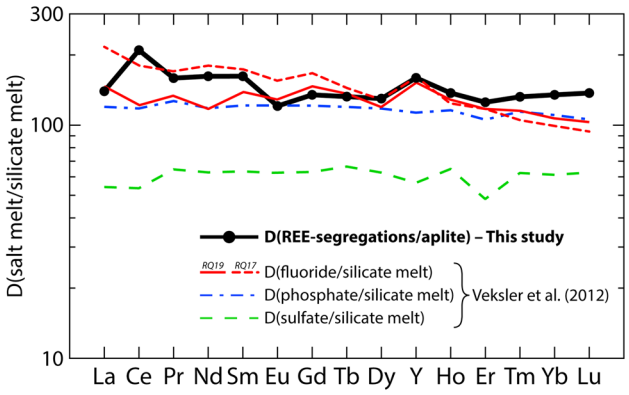

Fig. 6 Distribution coefficients D for REE and Y between the aplites and globular REE-rich segregations (black circles and heavy solid line; Table 3) compared to experimentally determined D values for silicate–fluoride (runs RQ-17 and RQ-19), silicate–phosphate (run C3-13) and silicate–sulfate melt immiscibility (Veksler et al. 2005, 2012)

solubility of SiO_2 in the F-rich phase, but relatively little F in the silicate-rich aplite (Table 3), which contrasts with the results obtained in this system by Veksler et al. (2005, 2012), but P_2O_5 is similarly distributed in both the natural and experimental systems.

Veksler et al. (2012) suggest that some of the variations in their experimentally determined distribution coefficients in the fluoride–silicate system, for example, Zr, Hf and Nb (Table 3), may reflect different starting melt compositions. The differences in D values in the natural and experimental systems for the elements noted above may also possibly reflect the significant differences in the compositions of the hypersolvus melts, which in the experimental systems involved on the one hand > 27 wt% F in a P_2O_5-free system, and on the other hand 30 wt% P_2O_5 in an F-free system, and with up to 10 wt% H_2O. The naturally occurring hypersolvus melt from which we propose that the aplite and globular REE-rich segregations separated contained much lower F and P_2O_5 (< 0.5 wt% each). Unfortunately, there are no experimental data available concerning immiscibility for $SiO_2 + F + P_2O_5$ mixtures to compare directly with the D values in the more complex natural system.

The naturally occurring hypersolvus melt also apparently contained little H_2O, much less than in the experimental systems, as indicated by its low LOI (Table 1), low abundance of biotite, and absence of both other hydrous phase in the aplites and of any aqueous fluid inclusions in either the aplite or the REE-rich segregations (Allaz et al. 2015). Further complicating the differences between the natural and experimental systems is the presence of small amounts of bastnäsite-(Ce), synchysite-(Ce), and pyrite in the REE-rich segregations (Allaz et al. 2015), indicating that the hypersolvus melt also contained a small amount of S and CO_2,

Table 3 D's determined from the natural system and experimental Si-P and Si-F systems

System	Natural[a]	Si-P	Si-F	Si-F	Si-F	Si-F
Run[b]		C3-13	C4-43	RQ-7	RQ-17	RQ-19
SiO_2	0.35	0.10	0.01	0.04	0.02	0.02
TiO_2	2.65	33.3	6.75			
Al_2O_3	0.33	0.89	1.65	0.99	1.41	1.52
Fe_2O_3	9.58	76.7	5.18			
MnO	29.4					
MgO	2.31	87.4	93.8			
CaO	4.08	102	69.2	94.8	121	99
Na_2O	0.02	5.95	2.58	4.18	2.83	2.95
K_2O	0.04	1.48	0.34	0.26	0.15	0.15
P_2O_5	22.1	17.3				
F	24.4		5.15	5.74	4.62	4.90
Cs	0.38	0.66	0.07			
Rb	0.12	0.78	0.12			
Ba	0.15	126	17.7			
Sr	0.76	122	29.6			
Nb	1.06	32.0	3.71	0.45	0.58	0.45
Zr	0.71	49.7	6.40	0.36	1.08	0.97
Hf	6.80	45.3	3.94	0.21	0.69	0.58
Th	114	67.8	49.0			
Pb	15.7					
U	69.0	57.8	13.0			
La	140	120	93.5	110	215	147
Ce	211	118	92.1	83.4	179	122
Pr	158	128	109	76.7	170	134
Nd	162	119	103	74.9	179	118
Sm	163	122	90.0	67.8	173	139
Eu	121	122	105	59.4	154	130
Gd	135	122	90.3	63.5	166	147
Tb	133	120	94.6	51.5	145	136
Dy	131	118	85.2	45.1	130	120
Y	160	114	103	60.2	161	153
Ho	137	117	89.4	42.1	125	129
Er	126	106	87.8	37.8	118	117
Tm	133	115	95.5	31.9	106	116
Yb	136	111	79.8	28.2	100	108
Lu	138	106	89.5	26.2	93.6	103

[a]*D* in the natural system calculated as the total segregations/aplites from Table 1

[b]Runs from Veksler et al. (2012)

which partitioned into the F-, P_2O_5- and REE-rich phase. It is unlikely that the small amount of carbonate in the hypersolvus melt affected the elemental distribution between the aplite and REE-rich segregations, since for carbonate–silicate immiscibility the REE concentrate into the silicate phase and D values vary significantly between LREE and HREE (Veksler et al. 2012). No experimentally determined D values for sulfide–silicate immiscibility have been published. In the natural system, $F + P_2O_5 + S$ were then further concentrated, possibly by a second stage of immiscible separation, into small rounded fluorite + monazite-rich blebs surrounded by pyrite (see Fig. 5 in Allaz et al. 2015), which occur within the cores of the REE-rich segregations.

Dolejš and Baker (2007a, b) investigated the compositional limits of fluoride–silicate liquid immiscibility in granitic systems and found that the miscibility gap was restricted to very high F contents. However, the naturally occurring hypersolvus melt from which we propose that the aplite and globular REE-rich segregations separated has low F content and is significantly different in composition than

a granite. Gramenitskii and Shchekina (1994, 2005) and Veksler et al. (2012) demonstrated that the region of liquid immiscibility in the fluoride–silicate system expands greatly in the presence of Li. We have not analyzed for Li, but have not observed any Li-bearing phases in either the aplite or REE-rich segregations.

Neither the aplite, REE-rich segregations nor the proposed hypersolvus magma from which they separated has a negative Eu anomaly, which precludes significant crystal-liquid fractionation involving plagioclase either at depth or during uprise of the hypersolvus magma. Its low H_2O and F content implies that to rise from lower crustal or upper mantle depths of > 45 km (see further discussion below) as a liquid, as suggested by our interpretation of the textural data (Fig. 1), it would have been relatively hot, the anhydrous liquid's temperature of andesitic magma at 15 GPa being > 1100 °C (Stern et al. 1975). Although there are no experimental data concerning the effects of pressure on immiscibility in the $SiO_2 + F + P_2O_5$ ($+ S + CO_2$) system, we speculate that pressure inhibits immiscibility, favoring the denser one-phase as opposed to the unmixed two-phase state, and that decompression played a significant role in maintaining the hypersolvus magma as a homogeneous liquid prior to its uprise, intrusion and cooling near the roof of the Longs Peak-St. Vrain batholith at approximately 6 km depth.

The origin of the H_2O-poor hypersolvus melt is uncertain. Calculated at 1422 Ma, the $\varepsilon_{Nd1.42Ga}$ values for the older quartz-feldspathic Idaho Springs Formation metamorphic rocks into which the Longs Peak-St. Vrain granite intruded average − 3.0, close to the range of the granites and consistent with similar metamorphic rocks possibly being the source from which the granites formed by partial melting (DePaolo 1981; Anderson and Thomas 1985; Smith et al. 1999). However, these values are not consistent with these upper crustal quartz-feldspathic metamorphic rocks being the source of the hypersovus magma from which the aplites and REE-rich segregations formed, since the latter have higher $\varepsilon_{Nd1.42Ga}$ values (Fig. 5).

These higher $\varepsilon_{Nd1.42Ga}$ values for the aplites and REE-rich segregations are interpreted as evidence either of a contribution to the hypersolvus magma of mafic mantle-derived melt, or anatectic melting of mafic rather than quartz-feldspathic crustal lithologies. The latter is an attractive possibility given that the presence of mafic xenoliths, entrained in the Devonian Colorado-Wyoming State Line kimberlites, demonstrate that the lower continental crust in this region is Paleoproterozoic in age and dominantly mafic in composition, consisting of two-pyroxene (± amphibole), two-pyroxene-garnet and clinopyroxene-garnet granulites (Bradley 1985; Farmer et al. 2005). In addition, the ε_{Nd} values at 1.4 Ga of the acid-leached mafic xenoliths (Farmer et al. 2005) overlap those of the aplite and REE segregations, ranging from − 2.7 to 0.6. The high $(La/Yb)_N$ of the hypersolvus magma also suggests greater proportion of garnet in the source compared to that of the granite, and the high Sr and lack of a negative Eu anomaly suggests that this source lacked significant amounts of plagioclase, also consistent with a lower crustal garnet granulite source. Similar mafic lower crustal lithologies have also been suggested as the source of F-rich Tertiary topaz rhyolites from the Western USA (Christiansen et al. 2007; Jacob et al. 2015). However, we also can not preclude a metasomatized, subcontinental mantle potential source for the hypersolvus granitic melt, as suggested for very large REE deposits elsewhere (Smith et al. 2016), given that mantle xenoliths entrained in the State Line diatremes suggest that a thick mantle lithospheric keel likely existed beneath this region during the Precambrian (Eggler et al. 1987).

Conclusions

Bowen (1928) concluded that "the association basalt-rhyolite, without intermediate types, cannot constitute a pair of immiscible liquids." However, he acknowledged the possibility of immiscibility in "highly specialized" silicate melt compositions. Veksler (2004) outlined experimental evidence for immiscibility in such specialized systems with high concentrations of B, F, Cl, P, C and S. The formation of quartz-tourmaline orbicules in S-type granites by the separation of an immiscible hydrous borosilicate melt from the granitic host magmas is an example where immiscibility has been invoked to explain the formation of some unusual orbicular, globular, and or ellipsoidal-shaped petrologic features observed in igneous rocks (Sinclair and Richardson 1992; Trumbull et al. 2008; Drivenes et al. 2015). The F-, REE-, and HFSE-rich ellipsoidal-shaped inclusion in the peralkaline Strange Lake granite pluton, Canada, is another example, this being attributed to silicate–fluoride melt immiscibility (Vasyukova and Williams-Jones 2016).

Here we suggest that the unusual F-, P-, and REE-rich globular segregations in aplite dikes within the Longs Peak-St. Vrain granitic pluton near Jamestown, Colorado, also have formed by silicate–fluoride + phosphate ($+ S + CO_2$) liquid immiscibility from an initially homogeneous hypersolvus silicate magma as it intruded, cooled and decompressed near the roof of this pluton. This suggestion hinges in large part on our interpretation of the textural evidence (Fig. 1) for the aplites and the REE-rich segregations having been co-existing liquids at the time of their cooling and crystallization.

The aplites and REE-rich segregations, neither of which have been recrystallized or chemically modified by subsequent hydrothermal alteration, deformation, uplift and exposure, provide a unique opportunity to compare D values of REE between naturally occurring immiscible fractions with those determined experimentally by Veksler et al.

(2005, 2012). Veksler et al. (2005, 2012) demonstrated that silicate–fluoride and silicate–phosphate immiscibility can increase the REE concentration in the F- and P_2O_5-rich relative to the silicate-rich immiscible fraction by greater than two orders of magnitude. D values for REE determined from the naturally occurring samples we have described are similar to those determined by Veksler et al. (2012), although they reflect immiscible segregation of melts in a more complex $F + P_2O_5 + S + CO_2$-bearing system, for which no experimental data are available. Nevertheless, they support the suggestion that immiscibility may play a significant role in concentrating REE to potentially economic values in magmatic systems.

Acknowledgements We thank P. Emery, T. Nystrom, and H. Scott from the Balarat Outdoor Education Center, Denver Public Schools, for providing access to the site, E. Anderson for assistance with data analysis, and also I. Veksler and O. Vasyukova for their helpful reviews of the manuscript. This work was supported by United States Geological Survey Mineral Resource External Research Program grant #G14AP00052.

References

Affholter KA (1987) Synthesis and crystal chemistry of lanthanide allanites. PhD dissertation, Virginia Polytechnic Institute and State University

Affholter KA, Adams IW (1987) Thermal breakdown of allanite to britholite. GSA Abstracts Progr 19:567

Allaz J, Persson PM, Raschke MB, Stern CR (2015) Proterozoic fluorbritholite-bearing REE-rich hydrothermal pods and veins from near Jamestown, CO. Am Mineral 100:2123–2140

Anderson JL, Thomas WM (1985) Proterozoic anorogenic two-mica granites: Silver Plume and St. Vrain batholiths of Colorado. Geology 13(3):177–180

Baker F, Hedge CE, Millard HTJ, O'Neil JR (1976) Pikes Peak batholith: geochemistry of some minor elements and isotopes, and implications for magma genesis. In Professional Contributions of Colorado School of Mines. Stud Colorado Field Geol 8:44–56

Bowen NL (1928) The evolution of the igneous rocks. Princeton University Press, Princeton

Bradley S (1985) Granulite facies and related xenoliths from Colorado-Wyoming kimberlites. MSc Dissertation, Colorado State University

Chakhmouradian AR, Wall F (2012) Rare earth elements: minerals, mines, magnets (and more). Elements 8:333–340

Chakhmouradian AR, Zaitsev AN (2012) Rare earth mineralization in igneous rocks: sources and processes. Elements 8:347–353

Christiansen E, Haapala I, Hart G (2007) Are Cenozoic topaz rhyolites the erupted equivalents of Proterozoic rapakivi granites? Examples from the western United States and Finland. Lithos 97:219–246

Cole JC, Braddock WA, Colorado N-C (2009) Geologic Map of the Estes Park 30′ × 60′ Quadrangle. US Geol Survey Sci Investig Map 3039:1

DePaolo DJ (1981) Neodymium isotopes in the Colorado Front Range and crust-mantle evolution in the Proterozoic. Nature 291:193–196

Dolejš D, Baker DR (2007a) Liquidus equilibria in the system K_2O–Na_2O–Al_2O_3–SiO_2–F_2O_1–H_2O to 100 MPa: I. Silicate–fluoride liquid immiscibility in anhydrous systems. J Petrol 48:785–806

Dolejš D, Baker DR (2007b) Liquidus equilibria in the system K_2O–Na_2O–Al_2O3–SiO_2–F_2O_{-1}–H_2O to 100 MPa: II. Differentiation paths of fluorosilicic magmas in hydrous systems. J Petrol 48:807–828

Drivenes K, Larsen RB, Müller A, Sørensen BE, Wiedenbeck M, Raanes MP (2015) Late-magmatic immiscibility during batholith formation: assessment of B isotopes and trace elements in tourmaline from the Land's End granite, SW England. Contrib Mineral Petrol 169: https://doi.org/10.1007/s00410-015-1151-6

Eggler DH, Meen JK, Welt F, Dudas FO, Furlong KP, McCallum ME, Carlson RW (1987) Tectonomagmatism of the Wyoming Province, Colorado. School Mines Quart 82:25–40

Farmer GL, Broxton ED, Warren RG, Pickthon W (1991) Nd, Sr, and O isotopic variations in metaluminous ash-flow tuffs and related volcanic rocks at Timber Mountain/Oasis Valley Caldera, Complex, SW Nevada: implication for the origin and evolution of large-volume silicic magma bodies. Contrib Mineral Petrol 109:53–68

Gay P (1957) An X-ray investigation of some rare-earth silicates: cerite, lessingite, beckelite, britholite, and stillwellite. Mineral Mag 31(237):455–468

Goddard EN, Glass JJ (1940) Deposits of radioactive cerite near Jamestown, Colorado. Am Mineral 25(6):381–404

Gramenitskiy EN, Shchekina TI (1994) Phase relationships in the liquidus part of a graniticsystem containing fluorine. Geochem Int 31:52–70

Gramenitskiy EN, Shchekina TI (2005) Behavior of rare earth elements and yttrium during the final differentiation stages of fluorine-bearing magmas. Geochem Int 43:39–52

Gysi A, William-Jones AE, Collins P (2016) Lithogeochemical vectors for hydrothermal processes in the Strange Lake peralkaline granitic REE-Zr-Nb deposit. Econ Geol 111:1241–1276

Jacob KH, Farmer GL, Buchwaldt R, Bowring SA (2015) Deep crustal anatexis, magma mixing, and the generation of epizonal plutons in the Southern Rocky Mountains, Colorado. Contrib Mineral Petro 169: https://doi.org/10.1007/s00410-014-1094-3

Klemme S (2004) Evidence for fluoride melts in Earth's mantle formed by liquid immiscibility. Geol 32:441–444

Klemme S (2005) Evidence for fluoride melts in Earth's mantle formed by liquid immiscibility: Comment and Reply: Reply. Geol 33:77

Peretyazhko IS, Zagorsky VY, Tsareva EA, Sapozhinikov AN (2007) Immiscibility of calcium fluoride and alumino-silicate melts in ongonites from the Ary-Bulak intrusion, Eastern Transbaikal region. Doklady Earth Sci 413:315–320

Peterman ZE, Hedge CE (1968) Chronology of Precambrian events in the Front Range, Colorado. Canad J Earth Sci 5:749–756

Peterman ZE, Hedge CE, Braddock W (1968) Age of Precambrian Events in the Northeastern Front Range, Colorado. J Geophy Res 73(6):2277–2296

Rabbitt JC (1952) Summary of the research work of the trace elements section geochemistry and petrology branch for the period July 1 - September 30, 1951. US Geol Surv report TEI-182

Sinclair WD, Richardson JM (1992) Quartz–tourmaline orbicules in the Seagull Batholith, Yukon Territory. Canad Mineral 30:923–935

Smith DR, Noblett J, Wobu RA, Unruh D, Douglass J, Beane R, Davis C, Goldman S, Kay G, Gustavson B, Saltoun B, Stewart J (1999) Petrology and geochemistry of late-stage intrusions of the A-type, mid-Proterozoic Pikes Peak batholith (Central Colorado, USA): implications for petrogenetic models. Precamb Res 98:271–305

Smith MP, Moore K, Kavecsánszki D, Finch AA, Kynicky J, Wall F (2016) From mantle to critical zone: a review of large and giant sized deposits of the rare earth elements. Geosci Front 7:315–334

Stern CR, Huang WL, Wyllie PJ (1975) Basalt-andesite-rhyolite-H2O: crystallization intervals with excess H_20 and H_20-undersaturated

liquidus surfaces to 35 kilobars, with implications for magma genesis. Earth Planet Sci Letts 28:189–196

Trumbull RB, Krienitz MS, Gottesmann B, Wiedenbeck M (2008) Chemical and boron-isotope variations in tourmalines from an S-type granite and its source rocks: the Erongo granite and tourmalinites in the Damara Belt, Namibia. Contrib Mineral Petrol 155:1–18

Tweto O (1979) Geologic map of Colorado, special publication, scale 1:500,000. U.S. Geological Survey, Reston

Vasyukova O, Williams-Jones AE (2014) Fluoride–silicate melt immiscibility and its role in REE ore formation: evidence from the Strange Lake rare metal deposit, Québec-Labrador, Canada. Geochim Cosmochom Acta 139:110–130

Vasyukova O, Williams-Jones AE (2016) The evolution of immiscible silicate and fluoride melts: implications for REE ore-genesis. Geochim Cosmochim Acta 172:205–224

Veksler IV (2004) Liquid immiscibility and its role at the magmatic–hydrothermal transition: a summary of experimental studies. Chem Geol 210:7–31

Veksler IV, Dorfman AM, Kamanetsky M, Dulski P, Dingwell DB (2005) Partitioning of lanthanides and Y between immiscible silicate and fluoride melts, fluorite and cryolite and the origin of the lanthanide tetrad effect in igneous rocks. Geochim Cosmochim Acta 69:2847–2860

Veksler IV, Dorfman AM, Dulski P, Kamenetsky VS, Danyushevesky LV, Jeffries T, Dingwell DB (2012) Partitioning of elements between silicate melt and immiscible fluoride, chloride, carbonate, phosphate and sulfate melts, with implications to the origin of natrocarbonatite. Geochim Cosmochim Acta 79:20–40